REVIEW

National Science Review
5: 653–672, 2018
doi: 10.1093/nsr/nwy077
Advance access publication 2 August 2018

CHEMISTRY

Special Topic: Single-Atom Catalysts

Single-atom catalyst: a rising star for green synthesis of fine chemicals

Leilei Zhang[1,†], Yujing Ren[1,2,†], Wengang Liu[1,2,†], Aiqin Wang[1,*] and Tao Zhang[1,*]

ABSTRACT

The green synthesis of fine chemicals calls for a new generation of efficient and robust catalysts. Single-atom catalysts (SACs), in which all metal species are atomically dispersed on a solid support, and which often consist of well-defined mononuclear active sites, are expected to bridge homogeneous and heterogeneous catalysts for liquid-phase organic transformations. This review summarizes major advances in the SAC-catalysed green synthesis of fine chemicals in the past several years, with a focus on the catalytic activity, selectivity and reusability of SACs in various organic reactions. The relationship between catalytic performance and the active site structure is discussed in terms of the valence state, coordination environment and anchoring chemistry of single atoms to the support, in an effort to guide the rational design of SACs in this special area, which has traditionally been dominated by homogeneous catalysis. Finally, the challenges remaining in this research area are discussed and possible future research directions are proposed.

Keywords: single-atom catalysts, fine chemicals, green synthesis, structure–reactivity relationship, heterogeneous catalysis

[1]State Key Laboratory of Catalysis, Dalian Institute of Chemical Physics, Chinese Academy of Sciences, Dalian 116023, China and [2]University of Chinese Academy of Sciences, Beijing 100049, China

*Corresponding authors. E-mails: aqwang@dicp.ac.cn; taozhang@dicp.ac.cn
†Equally contributed to this work.

Received 20 April 2018; **Revised** 24 June 2018; **Accepted** 31 July 2018

INTRODUCTION

Fine chemicals (<1000 tons/year) are important and valuable (>$10/kg) ingredients and intermediates for the manufacture of pharmaceuticals, agrochemicals and other specialty chemicals such as adhesives, sealants, dyestuffs, pigments, flavors, fragrances, food additives, biocides and corrosion inhibitors [1]. Due to their high purity, specialized nature, technology intensiveness and high added value, the manufacture of fine chemicals is always among the most active and strategic areas of the chemical industries [2].

Traditional synthetic routes for fine chemicals generally involve stoichiometric chemical reactions or use hazardous catalysts and thus produce serious environmental pollution and waste; the quantity of unwanted by-products may even exceed the amount of the desired products produced. Typical examples include the coupling of aromatic compounds with diazonium salts derived from stoichiometric amounts of nitrite salts to synthesize aromatic azo compounds [3] and the stoichiometric reduction of nitroarenes by iron metal to produce functional anilines [4]. With the increasing concern for the environment and safety, there is an urgent demand for the development of new, mild, efficient and straightforward methodologies and catalysts to achieve the green and sustainable synthesis of fine chemicals [5]. Such green strategies are characterized by several principles: atom-efficient catalytic processes, environmentally benign reagents and solvents, and one-pot tandem synthetic routes. On these grounds, a great number of efficient organometallic compounds and accompanying straightforward synthetic processes have been developed, which led to the flourishing of the fine chemical industry in the twentieth century, such as homogeneous Rh catalysts for hydroformylation reactions of olefins [6,7]. However, although these transition metal complexes exhibit high catalytic activity and selectivity, they are usually sensitive to moisture and/or air and are difficult to separate from

the products, which sometimes leads to the contamination of the products. With the rapid growth of nanoscience, heterogeneous catalysts, mainly supported transition metal nanoparticles, have been exploited to tackle these problems; however, their overall catalytic efficiencies are usually inferior to their homogeneous analogs. Therefore, the development of a new class of catalysts that integrates the merits of homogeneous and heterogeneous catalysts for the green synthesis of fine chemicals is highly desirable.

Single-atom catalysts (SACs) are defined as catalysts in which all of the active metal species exist as isolated single atoms stabilized by the support of or by alloying with another metal [8,9]. Since the seminal work of Zhang, Li, Liu and coworkers, who reported in 2011 that the Pt_1/FeO_x SAC was three times more active than its nano-Pt counterpart for CO oxidation [8], single-atom catalysis has become a new frontier in heterogeneous catalysis. SACs are distinguished from nanoparticle (NP) catalysts in that they do not contain metal–metal bonds and that the single metal atoms are usually positively charged. These unique geometric and electronic properties bring about significant alterations in the interactions with reactants/intermediates/products, leading to enhanced activity and/or selectivity, which are particularly desired for fine-chemicals production. Therefore, SACs are expected to combine the advantages of high catalytic activity, selectivity, stability and reusability for the green synthesis of fine chemicals. The past seven years have confirmed this expectation; a variety of SACs have been developed and have demonstrated excellent catalytic performance for various organic transformations, including selective hydrogenation, oxidation, hydroformylation and C–C coupling reactions. For example, FeO_x-supported Pt single-atom and pseudo-single-atom catalysts exhibited the best catalytic activity (at least 20-fold more active than any previously reported catalyst) and selectivity (∼99%) for the rather challenging selective hydrogenation of 3-nitrostyrene [10]; single-atom Rh_1/ZnO catalysts showed comparable activity to the benchmark homogeneous catalyst $RhCl(PPh_3)_3$ in the hydroformylation reaction of olefins [11]; and non-precious-metal Co(Fe)–N–C catalysts demonstrated 'platinum-like' performance for selective hydrogenation or oxidation reactions [12–18].

This review summarizes recent advances in SAC-catalysed organic reactions for the green synthesis of fine chemicals under liquid-phase reaction conditions—an area in which SACs are expected to find wide application and bridge homogeneous and heterogeneous catalysis. It should be mentioned that many of the examples discussed in this review are only simple model reactions, rather than real fine chemical substrates of intermediates. As preparation methods and characterization techniques for SACs have been described in detail in several recent excellent reviews [19–24], they are not emphasized in this review. The focus of this review is the catalytic performance of SACs in organic transformations as well as the coordination structure and oxidation state of the central single metal atoms. The stabilization mechanisms of the single atoms against leaching or aggregation in the liquid phase are also discussed. The aim of this review is to provide illustrative accounts of the recent progress in this research field and to extract fundamental principles to guide the rational design of SACs for green chemical synthesis.

SYNTHESIS OF FINE CHEMICALS PROMOTED BY SACS

SACs, with their well-defined mononuclear structures, have been expected to bridge homogeneous and heterogeneous catalysis since the term 'SAC' was first introduced in 2011 [8,9]. Over the past years, various supported SACs have been tested for a plethora of organic transformations, including selective hydrogenation of nitroarenes, ketones, alkynes and alkenes; selective oxidation of alcohols to aldehydes and ketones, of benzene to phenol and of silanes to silanols; hydroformylation of olefins; C–C coupling reactions; and biomass-related hydrodeoxygenation reactions. Compared with their NP counterparts, SACs afford enhanced activity by a factor of several to hundreds per metal atom and unparalleled selectivity in some reactions. The excellent stability of SACs provides additional advantages over their homogeneous analogs. While the active site structures of SACs may be less uniform than those of homogeneous catalysts due to their heterogeneous support surface, the well-defined structures arising from the coordination between single atoms and the support provide SACs with promising properties to mimic homogeneous catalysis in organic transformations.

Catalytic hydrogenation

Catalytic hydrogenations of unsaturated organic compounds represent one of the most important classes of chemical transformations and are widely applied in both the chemical industry and laboratory organic synthesis [25]. The majority of hydrogenation reactions involve the direct use of H_2 as the hydrogen source and are catalysed by VIII–X group metals such as Ni, Pd, Ru and Pt.

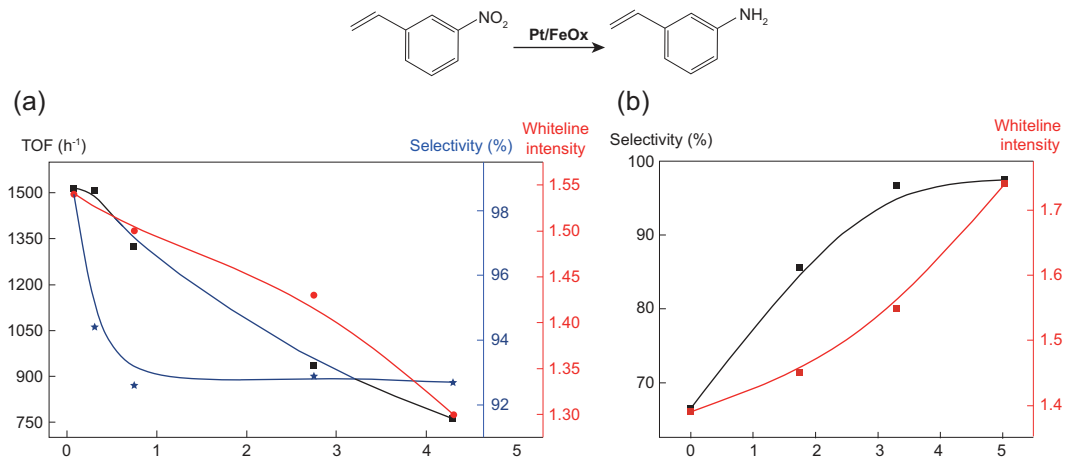

Figure 1. The dependence of activity/selectivity on the Pt content of the Pt/FeO_x catalysts (a) and on the Na content of the Na-2.16%Pt/FeO_x catalysts (b) for the chemoselective hydrogenation of 3-nitrostyrene, as well as the correlation between activity/selectivity and the oxidation state (white-line intensity) of Pt in the two systems.

The manufacture of functional anilines is of great significance in the chemical industry due to their versatility in biologically active natural products, agrochemicals, pharmaceuticals, dyes and ligands of organometallic complexes [4,26,27]. Compared with traditional synthetic methodologies (e.g. reduction by the transition metals iron and tin), catalytic hydrogenation is more efficient and environmentally benign. However, when one or more reducible organic groups (e.g. C = C) are present on the aryl ring containing the nitro group, the chemoselective hydrogenation of the nitro group is very challenging. Modification of the transition metal catalysts with proper additives achieved enhanced selectivity [28]; however, the catalytic activity was severely compromised. The hydrogenation of the nitro group is generally considered to be size-insensitive, whereas the reduction of the C = C group is highly sensitive to the size of the transition metal, with the reaction rate increasing with particle size [29]. Consequently, downsizing the active metal to its ultimate dispersion, namely single-atom dispersion, is expected to accomplish excellent chemoselectivity by suppressing the C = C double bond hydrogenation. Zhang, Wang and coworkers designed a FeO_x-supported Pt single/pseudo-single-atom catalyst. The term 'pseudo-single-atom catalyst' indicates a special structure composed of a few to tens of atoms that are loosely and randomly associated with each other, but do not form strong metallic bonds, and thus show structure and function similar to that of isolated single atoms. The catalyst was able to hydrogenate a broad scope of nitroarenes with different functional groups to the corresponding functionalized anilines with a turnover frequency (TOF) as high as 1514 h^{-1} and a chemoselectivity above 95% [10]. The loading of Pt on the FeO_x support had a significant effect on both the activity and chemoselectivity. As shown in Fig. 1a, both the activity per metal atom (TOF) and the chemoselectivity increased with decreasing Pt content until atomic dispersion was reached at 0.08 wt% Pt, at which the catalyst contained exclusively single atoms of Pt, and therefore achieved the highest activity and chemoselectivity (98.6% at a conversion of 96.5%). Interestingly, the white-line intensity of Pt in XANES (X-ray Adsorption Near-Edge Structure spectroscopy), which reflects the oxidation state of Pt, followed the same trend as the catalytic activity and chemoselectivity—that is, the higher the oxidation state, the higher the activity and chemoselectivity. This result indicated that the isolated, positively charged Pt on the FeO_x support acted as the main active site for the chemoselective hydrogenation of functionalized nitroarenes. Keeping this point in mind, and considering that the alkali metals could yield positively charged metal centers and also promote the dispersion of metal species [30,31], the same authors further tuned the electronic properties of the Pt center by introducing alkali metals to the high-Pt-loading catalyst (2.16 wt% Pt/FeO_x) [32]. By increasing the amount of Na to 5.03 wt%, the chemoselectivity increased remarkably from 66.4 to 97.4% (Fig. 1b); concurrently, the oxidation state of Pt increased as well. Moreover, detailed EXAFS (extended X-ray absorption fine structure) data analysis reveals that the structure of the central Pt sites changes with varying the amount of sodium; the Pt–Pt contribution decreases while the Pt–O contribution increases. Consistently with this trend, HAADF-STEM (high angle annular dark field scanning transmission electron microscopy) images clearly show that the Pt particles in the Na-containing samples all featured

abundant dark regions, which are probably due to lighter elements such as Na and Fe. In combination with the ^{57}Fe Mössbauer spectroscopy result that the $NaFeO_2$ species forms in the Na-containing sample, the authors proposed that the active sites were likely Pt–O–Na–O–Fe species. This scenario is reminiscent of that of a homogeneous catalyst, if the Na–O–Fe surrounding the single-atom Pt center is viewed as a robust ligand bridged by oxygen. Due to the higher contribution from Pt–O bonding than Pt–Pt bonding, the performance of this Na-modified Pt/FeO_x catalyst is quite similar to that of the SAC in terms of activity and selectivity. Nevertheless, in comparison to the SACs with relatively low metal loading, (e.g. 0.08% Pt/FeO_x), the high-metal-loading Na-modified Pt/FeO_x catalysts afforded a more than 20-fold increase in the productivity (activity per catalyst mass, rather than per Pt), which is of high importance in practical applications. In order to make the process more environmentally benign, the authors further studied the reaction in a CO_2-expanded toluene/THF system. The results showed that both the conversion and chemoselectivity could reach above 95% over Pt/FeO_x SAC, while the amount of the solvent toluene could be reduced by 90% in the CO_2-expanded toluene system [33].

It is noted that, even with the same single-atom dispersion and the same support, the activity and chemoselectivity of an SAC may vary depending on the intrinsic properties of the metal used. For example, while both Pt_1/FeO_x and Ir_1/FeO_x SACs are highly chemoselective towards the hydrogenation of 3-nitrostyrene to 3-aminostyrene, the Pd/FeO_x SAC is poorly selective (selectivity lower than 20%) for this reaction due to the intrinsically high activity of Pd towards the hydrogenation of C = C bonds [10]. Similarly, Zhang *et al.* found that sub-nanometric Pd clusters supported on CeO_2 nanorods were highly active (TOF as high as 44 059 h^{-1}) for hydrogenation of 4-nitrophenol and chemoselective for a broad scope of nitroarenes containing –OH, –X, –C = O and –CN groups, but poorly selective for substrates possessing a –C = C group [34]. It would be highly interesting to engineer the metal–support interaction to develop a new Pd SAC that is both highly active and chemoselective for the hydrogenation of nitro-styrenes.

The reaction mechanism of the chemoselective hydrogenation of nitroarenes over SACs has yet to be clarified. The results of control experiments involving the competitive adsorption of nitrobenzene and styrene revealed that the unique selectivity of SACs is not due to their intrinsically low activity for styrene hydrogenation, but instead due to the favorable adsorption of the nitro group in the presence of –C = C group [10], which is similar to the case behavior of the nanogold catalyst as well as the TiO_2-decorated nano-Pt catalyst [29,35]. Based on Fourier transform infrared spectroscopy (FT-IR) and density functional theory (DFT) theoretical studies [36], the nitro group is preferentially adsorbed on the support; the oxygen vacancies on the support surface (e.g. reducible supports like FeO_x and CeO_2) or the basicity of the support (e.g. the addition of Na increases the basicity of the support in the above-mentioned work) facilitate the preferential adsorption of the nitro group. This interaction can be understood in terms of Lewis acid–base interactions. The oxygen atoms in the nitro group are Lewis bases, while the oxygen vacancies of the reducible support act as Lewis acids; this ensures the strong and preferential adsorption of the nitro groups on the support surface, even in the presence of other reducible groups. Additionally, hydrogen can be easily dissociated at the isolated Pt (or other noble metal) single atoms, and the hydrogenation reaction probably occurs at the interface between the single metal atoms and the support, as illustrated in Fig. 2a. Nevertheless, this mechanism cannot completely justify the key role of single atoms in governing the high chemoselectivity. Alternatively, the nitro group could be adsorbed at the interface of the single metal atom and the support via the interaction of its two oxygen atoms with both the single metal atom and a nearby support cation, as illustrated in Fig. 2b. In either of the plausible scenarios above, the key point to be underscored is that the isolated and positively charged metal centers can successfully suppress the adsorption of C = C bonds, which would occur easily on their nanoparticle counterparts. Therefore, the single-atom dispersion is of paramount importance to achieve the chemoselective hydrogenation of nitroarenes to anilines, although cooperation between the single metal atoms and the specific support is required. Achieving an atomic-scale understanding of the reaction mechanism will require combined spectroscopic and theoretical studies.

There are two reaction pathways for the nitroarene reduction: a direct pathway involving nitro-nitroso-hydroxylamine-aniline steps and a condensation pathway involving nitro-nitroso-hydroxylamine-azoxy-azo-hydrazo-aniline steps [37]. In the above SAC systems, steric hindrance should prevent the reaction from proceeding via the condensation pathway, which requires the adsorption of two nitroarene molecules. However, in some cases, the azo is the desired product rather than the aniline, because aromatic azo compounds, with their great diversity of structures, represent the most widely used class of synthetic organic colorants by far [3]. For this purpose, Wang, Zhang and

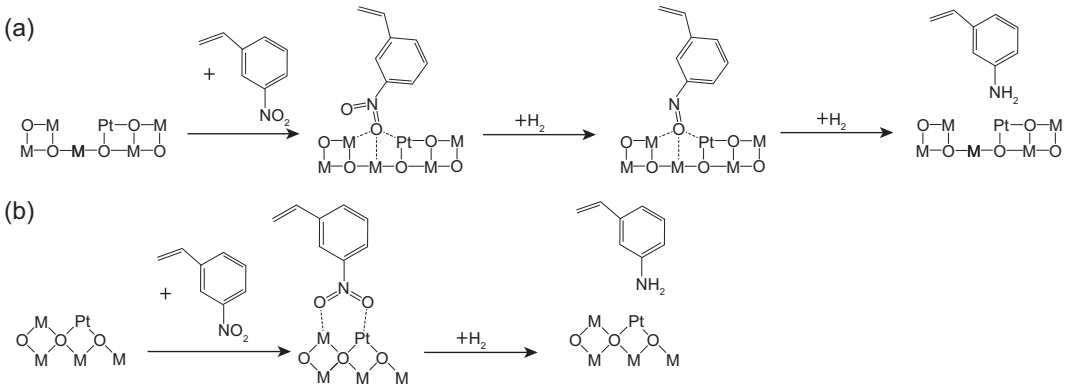

Figure 2. Two possible scenarios for the hydrogenation mechanism of nitroarenes on Pt-SACs with a reducible support.

coworkers explored atomically dispersed Co–N–C catalysts for the direct synthesis of azo compounds from nitroarenes [12]. The synthesis of this type of SACs involved the impregnation of a Co, N, C-containing precursor (e.g. a Co^{2+} phenanthroline complex) on a basic support (e.g. $Mg(OH)_2$) followed by pyrolysis at 600–800°C and etching with acid to remove the basic support as well as any particles of Co^0 or CoO_x. Extensive characterization with aberration-corrected HAADF-STEM, XAS (X-ray absorption spectroscopy) and XPS (X-ray photoelectron spectroscopy) in combination with DFT calculations revealed that the resulting material was a truly atomically dispersed catalyst in which cobalt existed exclusively as single atoms and was bonded strongly to four pyridinic N atoms within a deformed graphitic layer and weakly to two oxygen molecules in the axial direction, as shown in Fig. 3a and b. Differently from the rigid plane structure generally proposed in the literature [38], the deformed CoN_4C_8–$2O_2$ configuration might impart structural flexibility to the SACs similar to that of metal–ligand complexes and thus their catalytic activities may be comparable or even superior to that of their homogeneous analogs. In the hydrogenation of nitroarenes under mild conditions and in the presence of additional base (80°C, 3 MPa H_2, 1.5 h, *tert*-butyl alcohol as the solvent, catalyst loading of 0.7 mol% Co, 0.2 equivalents of NaOH), the Co–N–C SACs afforded good activity (TOF 35.9 h^{-1}) and excellent selectivity to azo compounds (Fig. 3c). Various functional groups including $–CH_3$, –C = C, $–CF_3$, –Cl, –Br and –I were tolerated in the reaction, and the catalyst could be reused without decay in the selectivity. The basic additive is the key to the condensation between nitrosobenzene and hydroxylamine to produce the target azo product; otherwise, anilines would be produced as the final product, as shown by the pioneering work of Beller and coworkers [39].

While the molecular-scale understanding of the reaction mechanism of these atomically dispersed Co–N–C catalysts has yet to be clarified, the $M–N_x$ motif (where M refers to transition metals such as Co, Fe, Ni, Cu, etc.) is probably the active site, even in the earlier reported Co_xO_y/N–C or Fe_xO_y/N–C systems [39,40]. To determine the real active species, Zhang *et al.* prepared a catalyst composed of metallic Co, Co_xO_y, Co_xC_y and CoN_x species using carbon as the support [41]. After acid etching, 78% of the Co-containing species had leached out and the residual Co species were encapsulated in thick graphitic nanoshells and thus inaccessible to any molecules, except for $Co–N_x$, which is stable against acid etching. Interestingly, the performance of the catalyst in the oxidative cross-coupling of primary and secondary alcohols remained the same, strongly suggesting that the atomically dispersed $M–N_x$ is the active site. This work also indicates that some complicated heterogeneous systems may need to be revisited to identify the real active sites by means of state-of-the-art characterization techniques.

For the hydrogenation reactions occurring on the SACs, one key question is how hydrogen molecules are activated on the single atoms. Recently, an increasing number of studies have suggested that H_2 is activated on SACs via a heterolytic pathway [42–45], which is quite different from the case of NP systems in which the homolytic dissociation of H_2 is favorable. For example, Zheng and coworkers reported a high-loading Pd_1/TiO_2 SAC that was obtained via a photochemical route on an ethylene glycolate (EG)-protected TiO_2 nanosheet material [42]. In their method, the EG radicals that were generated by ultraviolet (UV) radiation played a key role in producing and stabilizing the Pd single atoms at a relatively high loading (1.5 wt%). The coordination of the single Pd atoms with oxygen atoms from the EG molecule allowed the dissociation of H_2 in a heterolytic mode to produce $O–H^{\delta+}$ and $Pd–H^{\delta-}$ (Fig. 4), as proven by both kinetic isotope effect (KIE) and DFT calculations. The Pd_1/TiO_2 SAC exhibited high activity and stability for C = C and C = O hydrogenations; the TOF was enhanced

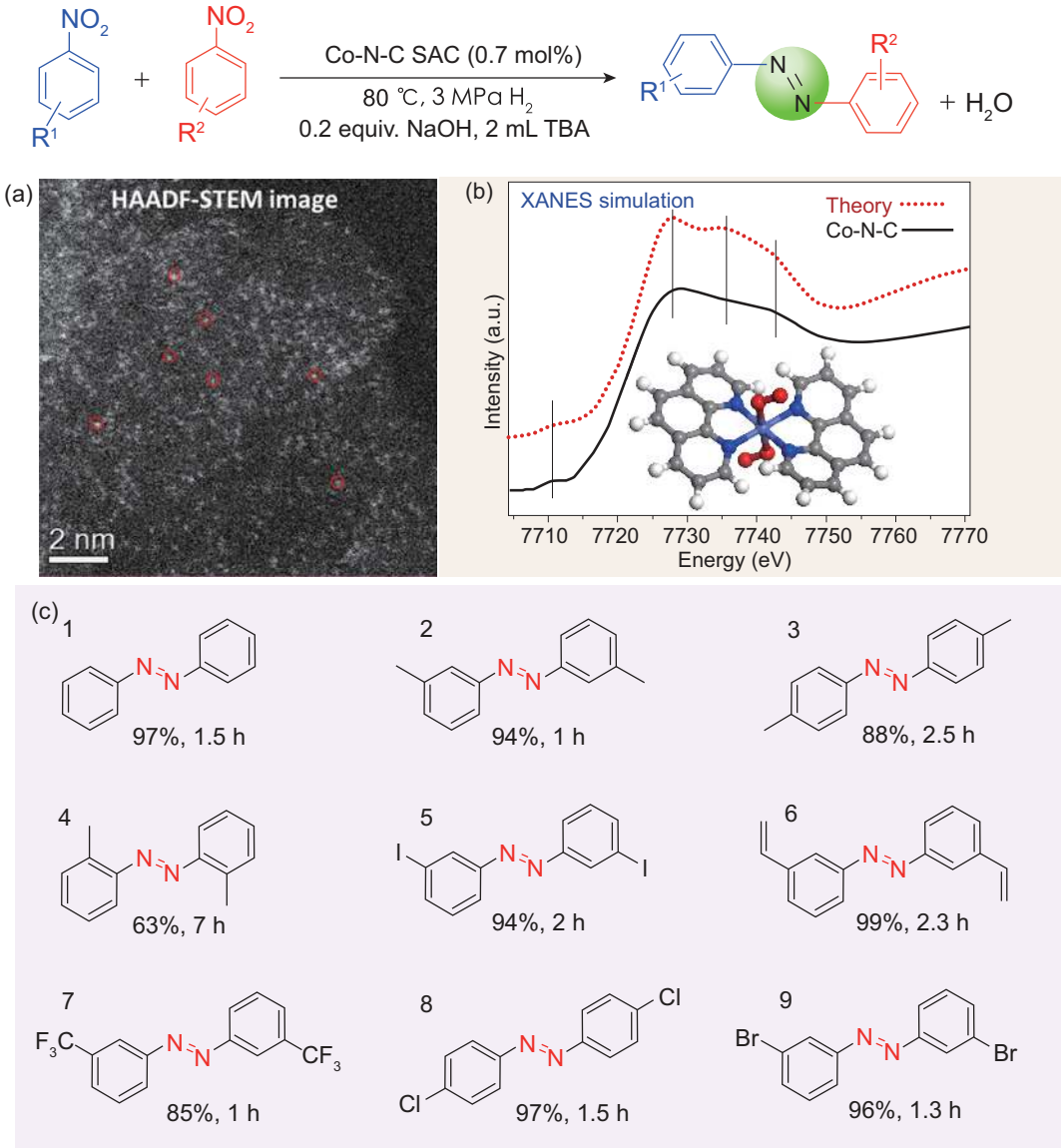

Figure 3. (a) HAADF-STEM image of the Co–N–C catalyst; (b) X-ray absorption spectroscopy (XAS) fitting and density functional theory (DFT) calculations of the Co–N–C catalyst; (c) substrate scope of the hydrogenation reaction on the Co–N–C catalyst. Adapted with permission from [12].

by a factor of 9 for styrene hydrogenation and a factor of 55 for aldehyde hydrogenation compared to the commercial Pd/C catalyst. The higher activity of the Pd_1/TiO_2 for the hydrogenation of polar unsaturated bonds probably originated from the heterolytic dissociation of H_2 at the Pd_1–O interface. Similarly, Yan and coworkers reported that single Pt_1 atoms anchored on active-carbon-supported phosphomolybdic acid (PMA) were more active for the hydrogenation of polar –C = O groups than of nonpolar –C = C groups, implying the heterolytic dissociation of hydrogen on the Pt_1–O_4 active sites [43]. In our recent work on the single/pseudo-single-atom catalyst Pt/WO_x, hydrogen was also found to dissociate in a heterolytic fashion at the interface of Pt and WO_x. The H^+ formed on WO_x and the H^- on the single Pt atom provided Brønsted acid sites and hydrogenation sites, respectively, for the concerted dehydration–hydrogenation reaction of glycerol to produce 1,3-propanediol [44], as shown in Fig. 5. Moreover, the introduction of single gold atoms to this Pt/WO_x system further promoted the heterolytic dissociation of H_2, possibly by modulating the interaction between Pt and WO_x, leading to remarkably enhanced activity and chemoselectivity towards 1,3-propanediol [45].

The heterolytic dissociation of H_2 favored on SACs is reminiscent of that of frustrated Lewis pairs (FLPs) in homogeneous catalysts, where H_2 is heterolytically dissociated at the sterically

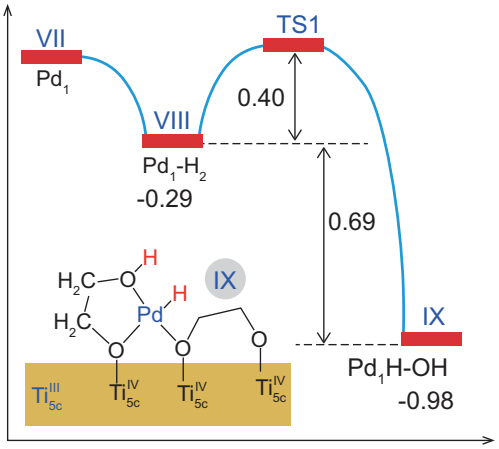

Figure 4. Energies and a model of the intermediates and transition states in the heterolytic H_2 activation process of Pd_1/TiO_2. Adapted with permission from [42].

encumbered Lewis acids and bases [46]. In supported SACs, the single metal atoms are usually positively charged and therefore act as a Lewis acid, while the nearby oxygen or nitrogen atoms from the support can act as a Lewis base; the combination of the two facilitates the dissociation of hydrogen via a heterolytic pathway.

SACs not only show higher activity than their NPs counterparts in catalysing the hydrogenation of polar unsaturated groups, but also catalyse the hydrogenation of alkynes with high selectivity towards alkenes. This kind of reaction was initially investigated on single-atom alloy (SAA) catalysts. The term SAA was first introduced by Sykes and coworkers [47]. SAA catalysts are special SACs in which the active metal atom (e.g. Pd) is isolated completely by the surrounding less active metal atoms (e.g. Cu). This configuration allows for the easy dissociation of hydrogen on the active single metal atoms and simultaneously weakens the binding of intermediates by spillover to the less active metal metals, thus accomplishing both high activity and high selectivity in the hydrogenation of alkynes to alkenes. Various combinations of SAA catalysts have been explored, such as Au–Pd [48], Ag–Pd [49], Cu–Pd [50], Zn–Pd [51], In–Pd [52] and Pt–Cu [53]. In addition to these SAAs, single Pd atoms on other supports have also been demonstrated to be effective [54–56]. For example, Perez-Ramirez and coworkers reported a Pt SAC supported on mesoporous polymeric graphitic carbon nitride (mpg–C_3N_4) that was 3 orders of magnitude more active than traditional NP catalysts (e.g. Au, Ag and CeO_2) in the hydrogenation of 1-hexyne, with 100% 1-hexene selectivity [56]. When the reaction was performed at 70°C and 5 bar H_2, [Pd]mpg–C_3N_4 was more active than

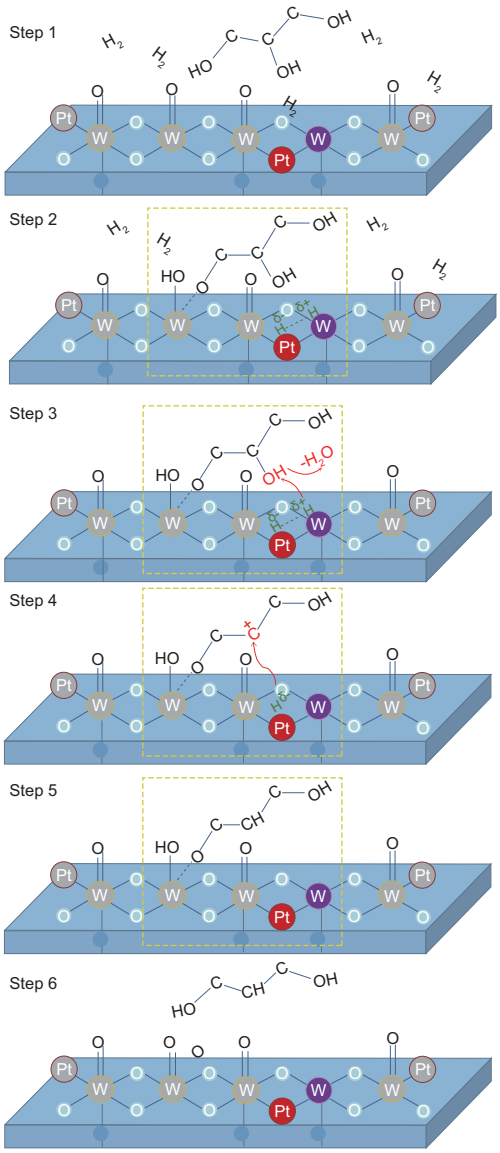

Figure 5. Proposed reaction scheme for the hydrogenolysis of glycerol to 1,3-PD over single-atom and pseudo-single-atom Pt/WO_x catalysts. Adapted with permission from [44].

$Pd–Pb/CaCO_3$ by a factor of 4, more selective than Pd/Al_2O_3 (90 vs 69%) and was as active as the Pd/TiS modified by ligands. Furthermore, no decrease in activity or selectivity was observed during 20 h of time-on-stream. Other substrates, such as 2-methyl-3-butyn-2-ol and 3-hexyne, could also be smoothly converted with excellent chemo- and stereo-selectivity (*cis*/*trans* ratio >20). DFT calculations revealed that hydrogen underwent heterolytic dissociation assisted by the support, leaving one H atom bonded to a N atom in the support and the second one to a Pd atom. When alkyne molecules were adsorbed, the semi-hydrogenation reaction proceeded smoothly and the alkene product was easily desorbed without over-hydrogenation or

oligomerization. The proposed reaction mechanism is quite similar to that of the gas-phase selective hydrogenation of acetylene to ethylene over Au(Ag, Cu) alloyed Pd SACs and Pd-Zn intermetallic compounds reported by Zhang and coworkers [48–51], in which ethylene was demonstrated to interact with the single Pd atoms via a weak π-bonding pattern, and could be readily desorbed without saturation.

Oxidation reaction

Selective oxidation is an important strategy for producing oxygenates, such as aldehydes, ketones or acid products, to be employed as building blocks in chemical processes that range from kilogram-scale applications in pharmaceuticals to 1000-ton-scale in chemicals. Traditional catalytic routes generally use expensive homogeneous complexes and are performed under harsh operating conditions, which bring about serious environmental issues and inevitable over-oxidation side reactions.

With the successful synthesis of SACs, a number of SACs have been explored in selective oxidation reactions and have shown promising catalytic performances. Pioneering work in this area was reported in 2007 by Lee and coworkers, in which a single-site Pd/Al_2O_3 catalyst showed 30 times greater catalytic activity (TOF: 4096–7080 h^{-1}) and selectivity (>91%) than its NP counterpart in the aerobic oxidation of allylic alcohols including cinnamyl alcohol, crotyl alcohol and benzyl alcohol [57]. This single-site Pd/Al_2O_3 catalyst was obtained by using mesoporous alumina as the support and an extremely low loading of Pd (0.03 wt%), both of which ensured the atomic dispersion of the Pd species. The isolated Pd^{II} surface species, which was identified using atomic-resolution HAADF-STEM, EXAFS and XANES, were proposed to be the active sites for the reaction. This catalyst also demonstrated impressive stability; the catalytic performance remained unchanged during the course of reaction over periods of days. This exceptional durability could be attributed to the high stability of the isolated Pd^{II} species, as well as that of the mesoporous structure of the support. Very recently, Li *et al.* reported an Au_1/CeO_2 SAC system that also showed excellent activity, selectivity and durability for the selective oxidation of alcohols to the corresponding aldehydes [58]. Based on isotopic exchange experiments, they proposed that the lattice oxygen from the CeO_2 support participated in the oxidation reaction, leading to the high selectivity towards aldehyde. The SAC system facilitated the removal and replenishment of the lattice oxygen by maximizing the interfacial sites between the single gold atoms and the CeO_2 support. In contrast, the gas-phase oxygen activation on the surface of gold NPs was less selective towards the aldehyde. Another important factor determining the selectivity is the adsorption of the aldehyde, which was found to be much weaker on the single atoms than on the NPs.

Toshima and coworkers constructed a 'crown-jewel'-structured Pd-alloyed Au SAC via replacing the Pd atoms at the top position of Pd_{147} particles with an Au atom [59]. The as-prepared catalysts showed excellent catalytic activity in the oxidation of glucose. The specific activity of the Au SAC was 20–30-fold higher than that of the Pd and Au mother clusters and 8–10 times those of the Pd/Au alloys with different Au/Pd ratios, although all had similar average particle sizes. The higher catalytic activity of the Pd-alloyed Au SAC than the Pd–Au alloys indicated position-dependent catalysis beyond the synergistic effects of Au and Pd, as the top atoms are assumed to be more active than the edge and face atoms owing to the more unsaturated coordination. To confirm this proposal, the authors prepared three Pd-alloyed Au SACs with different amounts of Au using the same method, in which Au would preferentially replace the top Pd atoms, then edge and lastly face Pd atoms. As the Au concentration was increased, the specific activity normalized to the Au mass decreased, which unambiguously demonstrated the lower activity of the edge and face Au atoms compared to that of top Au atoms. The Au 4f XPS spectra of the Pd-alloyed Au SACs showed a negative shift in binding energy compared with that of monometallic Au, indicating electron transfer from Pd to Au; thus, Au was negatively charged. The $Au^{\delta-}$ species could effectively donate electrons to O_2 to generate hydroperoxo-like species, which were considered to play an important role in the oxidation of glucose. Additionally, Tsukuda and coworkers reported a Pd_1Au_{24} SAC supported on a carbon nanotube (CNT) and investigated its catalytic performance in the aerobic oxidation of benzyl alcohol [60]. Compared with the monometallic Au_{25}/CNT, the single-Pd-atom-doped Pd_1Au_{24}/CNT exhibited significantly enhanced conversion of benzyl alcohol (from 22 to 74%). The synergistic effect between Au and Pd was attributed to electron transfer from Pd to Au, which promoted the activation of O_2. However, the selectivity of the catalyst was unsatisfactory and aldehyde, acid and ester products were produced with similar yields.

It should be noted that the oxidation mechanism on the single Pd atoms might be quite different from that on the single gold atoms or NPs. In the former case, the active oxygen mostly likely arises from the isolated PdO species and the Pd reduced during the reaction can be quickly re-oxidized by oxygen gas,

thus completing the redox cycle [57], while, in the latter case, oxygen is first activated on the electron-rich gold atoms to form O^{2-}, which then oxidizes the alcohol substrate [59].

In addition to noble metal SACs, atomically dispersed M–N–C catalysts have also been explored for aerobic oxidation reactions. In 2016, Davis's group reported a series of M–N–C SACs with non-noble metals, including Cr, Fe, Co, Ni and Cu, confined in a nitrogen-containing carbon matrix for the aerobic oxidation of alcohols in aqueous media [14]. Among these catalysts, Cu–N–C showed the highest catalytic activity for benzyl alcohol oxidation (TOF = 3.4×10^{-2} s^{-1}), followed by Co–N–C and Cr–N–C. The activity of Fe–N–C was lower than that of Cu–N–C by a factor of 50, although Fe–N–C is usually more active than Cu–N–C in the oxygen reduction reaction (ORR). KIE experiments were conducted to investigate the difference in catalytic activity between them. A large KIE effect (4.6) was observed on Fe–N–C, indicating that the elimination of β-H in benzyl alcohol was the rate-determining step, whereas a weaker KIE effect (2.2) was observed for Cu–N–C, suggesting Cu–N–C could abstract the β-H more easily. However, it should be noted that the as-prepared catalysts also contained nanoparticles encapsulated by carbon shells, whose role in the catalysis was not clearly determined.

Guan and coworkers also developed atomically dispersed Co SACs supported on nitrogen-doped graphene and investigated their catalytic behavior in the selective oxidation of alcohols [15]. The Co SAC exhibited excellent catalytic activity for a broad scope of substrates including aromatic and aliphatic alcohols, and moderate to excellent yields (54–92.4%) of the corresponding aldehydes were obtained. The base-free conditions and the use of air/oxygen as an oxidant seem attractive for practical application, although the organic solvent N,N-dimethylformamide (DMF) was used. Furthermore, some critical points, such as the doping effect of N in graphene, structure of the Co–N moiety and effect of calcination temperature, have yet to be clarified.

The selective oxidation of C–H bonds is a more demanding class of reactions than alcohol oxidation due to the high dissociation energy of C–H bonds and the over-oxidation side reactions [61]. Very recently, Liu *et al.* studied the selective oxidation of C–H bonds in aromatic and aliphatic hydrocarbons by using an atomically dispersed Fe–N–C catalyst [16]. By employing *tert*-butyl hydroperoxide (TBHP) as the oxidant, Fe–N–C SAC afforded excellent activity and selectivity even at room temperature, and a broad spectrum of substrates could be smoothly converted into the corresponding ketones. The performance was highly dependent on the pyrolysis temperature at which the SAC was derived from the $Fe(phen)_x$ (phen = 1,10-phenanthroline) precursor. Although the Fe–N–C catalysts obtained at different pyrolysis temperatures (ranging from 700 to 900°C) included almost exclusively or even exclusively atomically dispersed Fe species, their exact structures were rather complicated and in fact consisted of a mixture of FeN_x species (x = 4–6). The employment of the powerful ^{57}Fe Mössbauer spectroscopy technique allowed the identification and quantification of the different Fe centers. As shown in Fig. 6a, the relative concentration of each species differed with the pyrolysis temperature, and the most active species was the medium-spin FeN_5 site (D4 in Fig. 6a), which afforded a TOF of 6455 h^{-1} for the oxidation of ethylbenzene to acetophenone. This TOF was more than 1 order of magnitude higher than that of the high-spin FeN_6 species (D2) and low-spin FeN_6 species (D3), and even several times more active than the $Fe(II)N_4$ species (D1). The high activity of the FeN_5 structure was attributed to the unsaturated coordination of the Fe single atoms (actually Fe^{3+} cations), which provided adsorption sites for TBHP (H–O–O–, Fig. 6b). This behavior resembles the oxygen activation of the hemoglobin molecule [62]. In this aspect, the Fe–N–C SACs are expected to mimic the metalloenzymes in more important but complicated organic transformations. However, in the current Fe–N–C SACs, the most active species are unfortunately the least abundant (28% or less based on Fig. 6a). Evidently, there is plenty of room for future research in the design and synthesis of atomically dispersed single-site catalysts.

The direct catalytic conversion of benzene to phenol is a demanding and practically important reaction in the field of C–H activation. Bao and coworkers prepared a highly dispersed FeN_4/GN catalyst via the high-energy ball milling of iron phthalocyanine (FePc) and graphene nanosheets under controllable conditions [17]. The graphene-matrix-confined coordinatively unsaturated iron sites demonstrated excellent catalytic activity in the oxidation of benzene with H_2O_2 as the oxidant at room temperature. For example, the TOF value reached 84.7 h^{-1} and a phenol yield of 18.7% was obtained at a conversion of 23.4%. Notably, the reaction even proceeded efficiently at 0°C, reaching a phenol yield of 8.3% after 24 h of reaction. Furthermore, the catalyst could be reused six times without a decrease in its catalytic activity. *In situ* XAS and Moössbauer measurements were performed to investigate the catalytic mechanism. For the fresh catalyst, both the Fe K-edge XANES spectra and

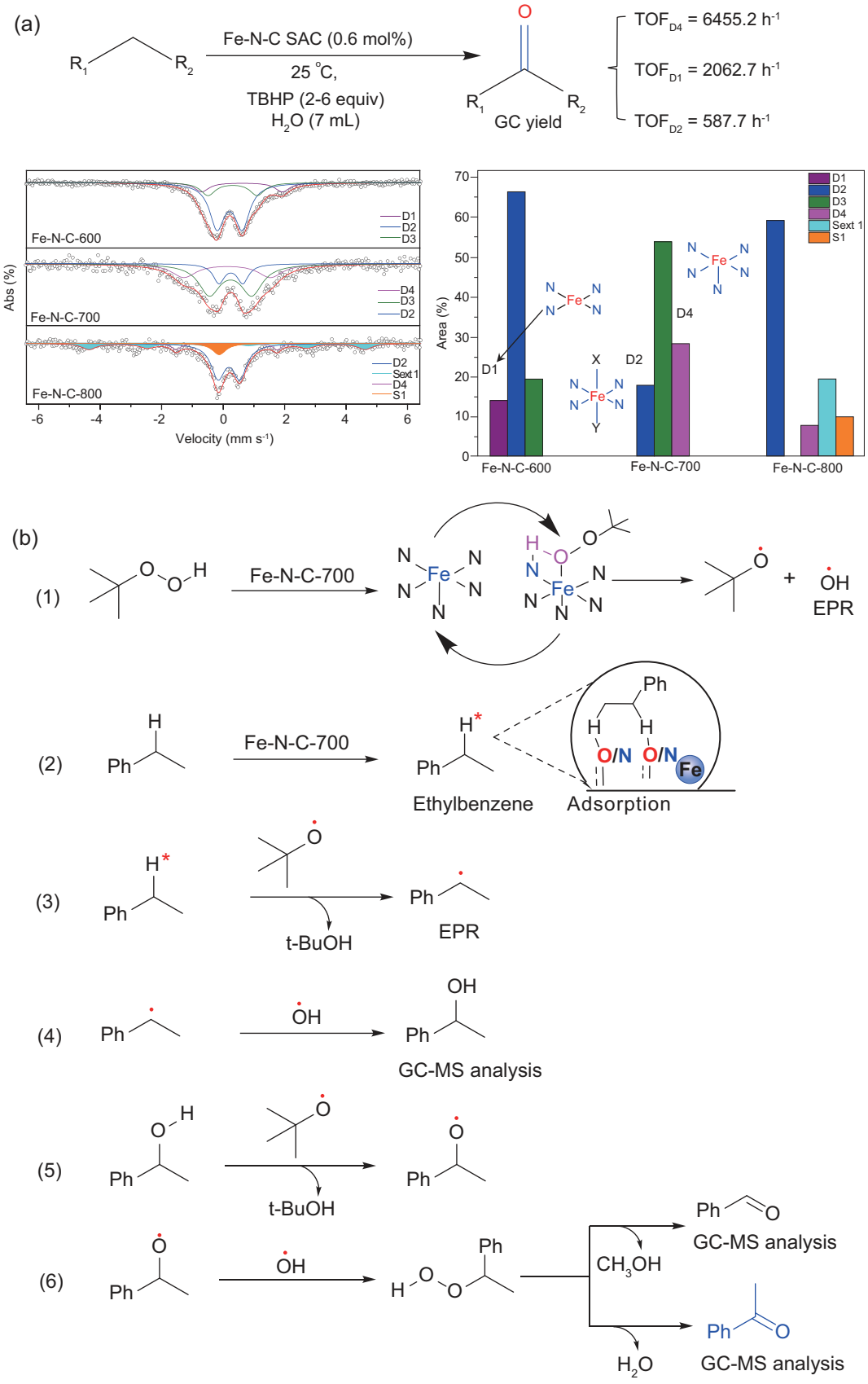

Figure 6. (a) ^{57}Fe Mössbauer spectra of the Fe—N—C-600/700/800 catalysts and the relative concentration of each species; (b) proposed reaction mechanism of ethylbenzene oxidation on the FeN_5 site. Adapted with permission from [16].

Fourier transformed EXAFS spectra in r-space were quite similar to that of FePc, indicating that the Fe in FeN_4/GN adopted the same FeN_4 structure, with Fe coordinated to four N atoms within a planar sheet, as that of FePc. Upon treatment with H_2O_2, the pre-edge peak in the Fe K-edge XANES spectra broadened and increased in intensity due to the formation of Fe = O. The intensity of the first strong peak in the FT-EXAFS spectra in r-space was also enhanced, suggesting that a sharp increase in the coordination of Fe resulted from the formation of Fe = O/O = Fe = O. ^{57}Fe Moössbauer measurements also revealed that the amount of Fe = O increased after H_2O_2 treatment and then decreased upon contact with benzene. These results, together with DFT calculations, showed that the single Fe atom was oxidized by H_2O_2 to form an O = Fe = O intermediate, which then oxidized benzene to form phenol.

Li *et al.* also constructed Fe–N–C SACs by the pyrolysis of metal hydroxides or oxides coated with polymers of dopamine, followed by acid leaching [18]. The obtained Fe–N–C SAC exhibited high catalytic activity for the hydroxylation of benzene to phenol (45% benzene conversion with 94% selectivity). Based on electron paramagnetic resonance (EPR) analysis and DFT calculations, they proposed a similar reaction mechanism to that of Bao, in which the H_2O_2 oxidant was activated on the single Fe atom, and the resulting Fe^{IV} = O species was considered to be the active intermediate in the reaction. Notably, although Fe–N_4 moieties were proposed as the active species in both works, the selectivity towards phenol (94%) in Li's report was higher than that of Bao's (∼80%), indicating that there might be some subtle discrepancy in the exact structure of the two active sites. Further efforts are expected to identify the active species using XAS and Moössbauer characterization and/or poisoning experiments. In addition, the use of a large excess of H_2O_2 as oxidant decreased the catalytic efficiency to some extent in both cases.

Silanols are important building blocks in polymer chemistry. The selective oxidation of silanes with water to synthesize silanols has attracted increasing attention for its safety (nonexplosive, nonflammable and nontoxic) and atomic economy (hydrogen gas as the only by-product) [63]. Chen and coworkers prepared Au SACs supported by mesoporous carbon graphitic carbon nitride (mpg–C_3N_4), which showed excellent catalytic performance in the oxidation of silanes by water [64]. Nevertheless, in comparison with the gold NPs supported on silica previously reported for the same reaction [65], the Au_1/C_3N_4 showed only comparable activity. One advantage of the Au_1/C_3N_4 SAC is its excellent stability; it could be recovered and reused at least 10 times with its activity and selectivity being maintained well. The characteristic coordination cavity surrounded by N atoms in the mpg–C_3N_4 could anchor and stabilize the Au single atoms; this effect was believed to contribute to the high durability of the catalyst.

Hydroformylation of olefins

The hydroformylation of olefins involves the addition of syngas (a mixture of CO and H_2) to olefins for the production of aldehydes and represents a typical example of an efficient and clean chemical process with 100% atom economy. The aldehydes are valuable final products and important intermediates for the synthesis of bulk chemicals such as alcohols, esters and amines; more than 10 million tons of aldehydes are manufactured per year globally [66]. Cobalt-based catalysts were the first generation of catalysts for these transformations; however, they required harsh reaction conditions and had low productivity. In 1968, a Rh-based catalyst [$RhCl(PPh_3)_3$] was reported by Wilkinson *et al.* [67], and was much more active and selective than the Co-based catalysts under mild reaction conditions, thus opening a new era of rhodium–alkylphosphine/phosphite complexes for the hydroformylation reaction [66]. The alkyl–phosphorous ligands, with their unique steric bulk and electron-donating effects, contribute greatly to the high activity and selectivity. However, these homogeneous complexes are difficult to recover. Thus, great efforts have been devoted to the heterogenization of Rh-based hydroformylation catalysts, including immobilization of the homogeneous complexes on a solid support by ion exchange, adsorption or covalent grafting [68]. However, the interaction between the post-heterogenization Rh metallorganics and the support is relatively weak. Degradation of the ligands and/or the Rh complexes tends to occur during the course of the reaction, which necessitates the periodic supplementation of the active components. Furthermore, only a low concentration of phosphorous ligands can be grafted onto the surface of the support using these methods, which usually results in poor catalytic activity, selectivity and stability because of the low P/Rh ratio [69,70].

Recently, the groups of Ding and Xiao groups have made great progress in the heterogenization of homogeneous Rh catalysts by designing porous organic ligands (POLs) to support Rh [71–73]. They chose the well-known electron-donating ligand triphenylphosphine (PPh_3) as the backbone of the monomer and grafted a vinyl group to the three benzene rings in PPh_3 to construct vinyl-functionalized PPh_3 (3V–PPh_3), which then

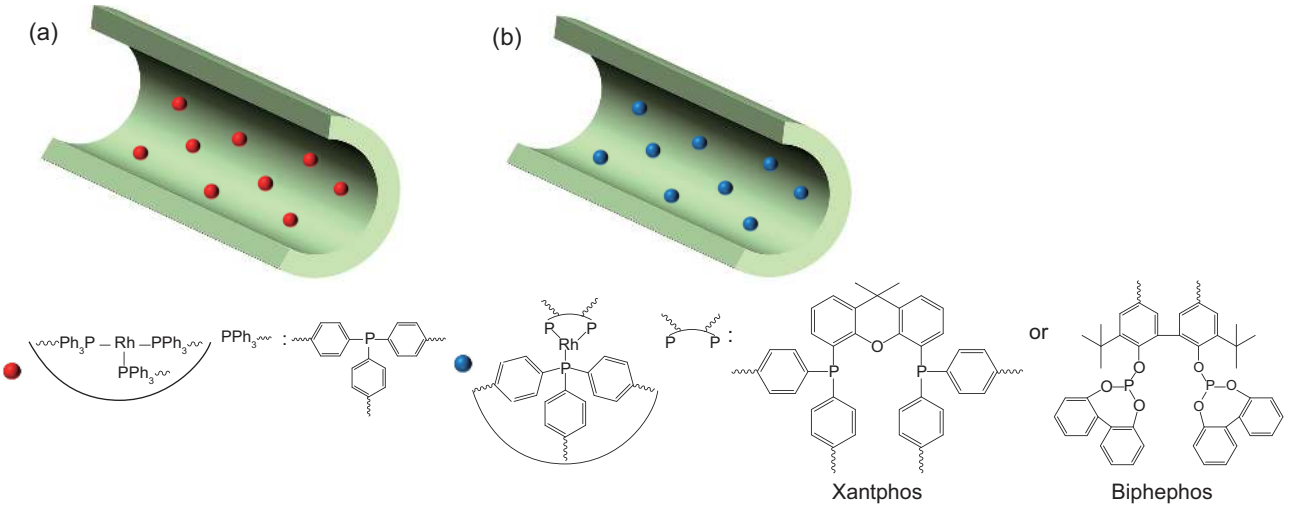

Figure 7. The proposed structures of the (a) Rh/POL–PPh_3 and (b) bidentate-ligand-doped Rh/POPs-PPh_3 catalysts.

underwent polymerization under solvothermal conditions to yield a porous organic polymer (POP) with high surface area and rich porosity (Fig. 7a). One of the most significant advantages of this method is that the PPh_3 moieties can be anchored with a high loading and are homogeneously distributed throughout the support via covalent bonding (C–C). This not only stabilizes the active Rh species exclusively as single atoms, but also ensures the high P/Rh ratio that is required for high catalytic activity and selectivity. In the hydroformylation of 1-dodecene, the conversion reached 86.4% with a high linear/branched aldehyde ratio (l/b = 6.6). The high selectivity towards linear aldehydes was thought to arise from the confinement effect of the micropores (0.7–1.5 nm) in the support. More impressively, in contrast to the vulnerability of most previously reported heterogenized molecular catalysts [68,74], the Rh SAC was quite stable for more than 500 h time-on-stream in continuous flow reaction, demonstrating its great potential for practical applications. However, the substrate tolerance of the catalyst was unsatisfactory and, for the hydroformylation of the shorter-chain substrate 1-octene, the linear/branched ratio was poor (45/55), and a large amount of isomerized alkene was produced. To improve the regio-selectivity, the authors doped bidentate ligands such as Xantphos, which was reported by Van Leuween [75], and biphephos, which was developed by the Union Carbide Corp. [76,77], onto the POP–PPh_3 (Fig. 7b). These bidentate ligands usually exhibit large natural bite angles (~120°) and, when coordinated with an Rh cation, the formed complex preferentially adopted a diequatorial rather than an equatorial-apical configuration, which led to an increase in the steric congestion around the Rh center and resulted in more selective formation of the sterically less demanding linear alkyl rhodium species and subsequently of the linear aldehydes [75]. Using a similar method, Ding and coworkers functionalized the Xantphos and biphephos ligands with vinyl groups, which then underwent co-polymerization with the 3V–PPh_3 to yield the support [78]. The Rh species in these catalysts still existed as single atoms. Compared with Rh/POP–3V–PPh_3, the Xantphos- and biphephos-doped catalysts afforded greatly enhanced regio-selectivity, although the catalytic activity was decreased to some extent, most likely due to the limited mass transfer. For example, the l/b ratio in the hydroformylation of 1-octene over Xantphos-doped Rh/POPs–PPh_3 increased from 45/50 to 90/10 and, in the hydroformylation of propene on biphephos-doped catalysts, the l/b ratio reached as high as 24.2. Impressively, the biphephos-doped catalyst was also effective for the isomerization–hydroformylation of internal olefins and the regio-selectivity for linear aldehyde reached up to 92%. The authors proposed that the PPh_3 ligands contributed mainly to the overall catalytic activity and stability owing to their strong electron-donating capacity and multiple binding with Rh cations, whereas the bidentate ligands were mainly responsible for the high regio-selectivity due to their steric hindrance. The POLs strategy developed by Ding and Xiao opened a new approach for the heterogenization of metallorganic molecular catalysts that could maintain their high activity and regio-selectivity while creating robustness. Nevertheless, the tedious procedures required to prepare the polymers and the use of expensive ligands and Grignard reagents represent barriers to their future industrial application. Further efforts must be devoted to developing facile and inexpensive synthetic routes and exploring other P-containing materials (e.g. MOFs, COFs) for such transformations.

Given the high cost and vulnerability of the phosphorous ligands, supported Rh NPs catalysts without P-ligands were developed for the hydroformylation of olefins; however, their catalytic performances were inferior to those of their homogeneous analogs [79]. SACs, in which the single metal atoms are coordinated to heteroatoms on the support, are regarded as a mimic of supported homogeneous catalysts and thus are expected to perform well in the hydroformylation of olefins. Indeed, the Rh SACs met some of the criteria for the hydroformylation of olefins. First, in most Rh homogeneous catalysts, Rh(I) species are considered to be the active sites; fortunately, Rh single atoms are generally positively charged. Second, Rh single atoms are reported to effectively activate both H_2 and CO, and the isolated Rh centers are believed to interact with olefins weakly without hydrogenation. Third, the confinement in some SACs is expected to have steric effects similar to those of bulky P-ligands. Recently, several exciting examples have demonstrated the feasibility of Rh SACs for the hydroformylation of olefins. Lang *et al.* fabricated a Rh_1/ZnO catalyst for the hydroformylation reaction [11]. They chose ZnO nanowires (ZnO-nw) as a support and a Rh SAC with a loading of 0.006 wt% was prepared. For comparison, ZnO-nw-supported Rh NPs were also synthesized. In the hydroformylation of styrene, when the Rh loading was decreased from 0.3 to 0.006 wt%, the turn over number (TON) increased from 7×10^3 to 4×10^4. Notably, the TONs of Rh_1/ZnO-nw were even higher than those of homogeneous $RhCl_3$ and Wilkinson's catalyst $RhCl(PPh_3)_3$ (TON = 3324 and 1.9×10^4, respectively). Moreover, the chemoselectivity of the Rh_1/ZnO-nw catalyst reached 99%, which was much higher than those of its homogeneous counterparts (83–92%). Almost no hydrogenation of olefins occurred on the catalyst, indicating that the single Rh atoms interacted with the olefins through a π-mode interaction, which was in good agreement with the behavior of other SACs for hydrogenation reactions [10,42,56]. Unfortunately, the Rh_1/ZnO-nw SAC did not exhibit regio-selectivity towards the linear aldehydes; the linear/branched ratio was about 1. Generally, high regio-selectivity can only be obtained when the Rh centers have significant steric hindrance during the insertion of CO. The unsatisfactory regio-selectivity of the Rh_1/ZnO-nw SAC may imply that the Rh center had low steric congestion. XPS and *in situ* XANES characterization results indicated that the single Rh atoms were in a nearly metallic state, which implied that the single Rh atoms might have been located atop a Zn atom. This position would leave the Rh single atoms open to CO insertion from every direction and thus lead to poor regio-selectivity.

However, high regio-selectivity and high activity over Rh SACs was achieved by fine-tuning the valence state and location of the single Rh atoms on the support, as demonstrated by Zeng and coworkers [80]. They constructed a Rh_1/CoO SAC by confining the single Rh atoms in the CoO layers via galvanic replacement between Rh(III) and CoO. Inductively coupled plasma atomic emission spectroscopy (ICP-AES) examination and HAADF-STEM images suggested that the single Rh atoms occupied the Co positions. In the liquid-phase hydroformylation of propene, the 0.2% Rh/CoO SAC achieved a TOF value of 2065 h^{-1}, which was even higher than that of Rh/POPs–PPh_3. Furthermore, the catalyst showed impressive chemoselectivity (>99%) and regio-selectivity for 1-butaldehyde (94.4%), higher than those of its nano-counterparts (68.7 and 53.9% for 1.0% Rh/CoO and 4.8% Rh/CoO). This high chemo- and regio-selectivity may arise from two features. First, XPS measurements demonstrated that the single Rh atoms were positively charged even under the reaction conditions, allowing the single Rh atoms to stably fill the Co(II) vacancies; that is, the Rh single atoms were coordinated to four oxygen atoms within the CoO layer in the equatorial direction of an octahedral configuration. Second, the single Rh atoms were confined within the CoO sheets, although according to DFT calculations, Rh moved 1.3 Å out of the plane during the reaction. This confinement limited the possible CO insertion pathways, which in turn preferentially yielded the linear aldehyde due to steric hindrance. Furthermore, the CoO support might have assisted in the activation of H_2 and CO, as in the case of Au/Co_3O_4 [81], which would increase the catalytic activity. This work subverted the traditional opinion that high regio-selectivity can only be obtained with the assistance of expensive phosphorous ligands, and demonstrated that the heteroatoms (e.g. O) in the support can fulfill the role of the bulky P-ligands in a carefully designed SAC.

C–C coupling reaction

The construction of C–C bonds, which is a vital method for the formation of complex molecules from simple substrates, is one of the central themes in modern synthetic chemistry. Typical powerful approaches include the Suzuki cross-coupling reaction [82], Heck reaction [83] and α-alkylation of enolates [84], which are generally catalysed by Pd, Ir or Pt complexes. When aryl halides are used as substrates, the chlorides are cheaper and more readily available than the bromides and iodides, but are more difficult to activate because of the higher

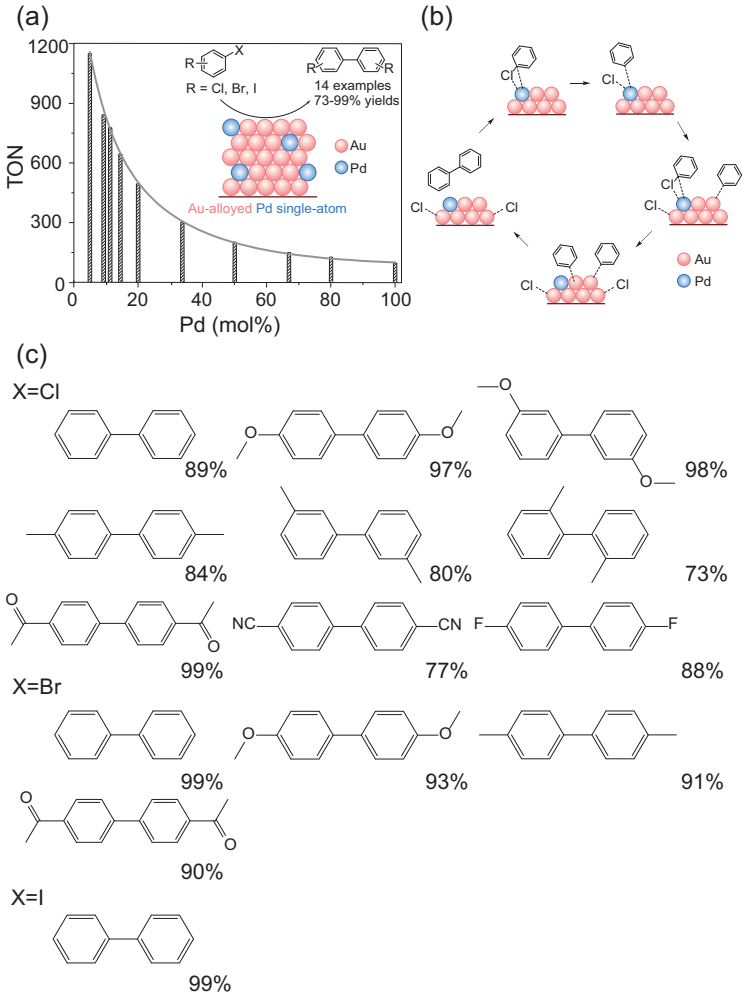

Figure 8. (a) Relationship between activity (turnover number, TON) and Pd concentration in the Au–Pd/resin catalysts for the Ullmann reaction of chlorobenzene; (b) proposed reaction mechanism; (c) substrate tolerance (the percentages in C indicate the product yield). Adapted with permission from [85].

dissociation energy of the C–Cl bond. Zhang *et al.* prepared an ion-exchange-resin-supported Au–Pd SAA catalyst that exhibited high catalytic activity and selectivity in the Ullmann reaction of aryl chlorides [85]. Both CO-DRIFTs (diffuse reflectance infrared Fourier transform spectroscopy) and EXAFS characterization confirmed the formation of an SAA structure at Au/Pd $\geq$ 6, with the Pd atoms isolated by the surrounding Au atoms. In the Ullmann reaction of chlorobenzene, an exponential increase of the TON (normalized by Pd mass) was observed with decreasing Pd concentration (Fig. 8a). This interesting trend can be rationalized by the assumption that, with an increase in the Au/Pd ratio, the Pd single atoms are mainly located at the edges and corner positions of the Au nanoparticles (Fig. 8b), which should be more active than those on facets because of the more unsaturated coordination environment, as in the case of the aforementioned 'crown-jewel'-structured Au SACs [59]. Furthermore, the catalyst exhibited promising substrate tolerance and durability for Ullmann reactions of aryl chlorides, bromides and iodides (Fig. 8c) and could be reused eight times without decay in their activity. Hot filtration experiments demonstrated a heterogeneous reaction mechanism. It was proposed that the Au in the catalysts not only played a role in separating Pd to form single atoms, but also promoted the dissociation of the C–Cl bond and the coupling of two aryl groups, thus opening a new method of fabricating efficient alloyed SACs for other reactions. Future work can be devoted to exploring other inexpensive transition metals to isolate Pd, in light of the high price of Au.

In addition to the SAA, a TiO_2-supported Pd SAC was also explored for the Sonogashira coupling reactions of aryl bromides and iodides with phenylacetylene [86]. The catalyst afforded complete conversion of phenylacetylene after reaction at 60°C for 3 h in the Sonogashira coupling reaction of phenylacetylene and iodobenzene, with the product selectivity reaching over 90%. The coupling reaction also proceeded readily for substituted phenylacetylenes with different functional groups and aryl bromides and iodides, and the corresponding products were obtained in high yields. However, for the more challenging aryl chloride substrates, the catalyst showed rather low activity. XAS and XPS characterization, in combination with DFT calculations, revealed a Pd_1O_4 structure in which the positively charged and isolated $Pd^{\delta+}$ species interact strongly with four surface lattice O atoms of the TiO_2 support. Such a structure provides multifunctional Pd, O_{ad} and Ti_{5c} atoms for the activation of the reactants, and therefore a lower apparent activation energy of 28.9 kJ/mol is required in comparison with that of the homogeneous catalyst $Pd(PPh_3)_2Cl_2$ (51.7 kJ/mol), demonstrating the concerted catalysis by the TiO_2 support and single Pd atoms.

Kim *et al.* reported a thiolated multiwalled nanotube (MWNT) supported Pt SAC that acted as a good catalyst for the Suzuki cross-coupling reaction of 4-iodoanisole and 4-methylbenzene boronic acid [87]. The Pt-S-MWNT SAC afforded a high product yield of 99.5%, which was much higher than that on Pd-S-MWNTs, Pd/C or H_2PtCl_6. However, for bromide and chloride, much lower yields of 10.4 and 4.8% were obtained, respectively. The catalyst could be recovered by filtration and could be reused 12 times without significant decrease in the yield. XANES spectra showed a white-line intensity slightly higher than that of Pt foil, but much lower than that of H_2PtCl_6, suggesting that the single Pt single atoms were positively charged. The positively charged single Pt atoms could easily dissociate the

C–I bond and were believed to be responsible for the high activity. It was also noted that, in the Pt-S-MWNT SACs, the single Pt atoms were coordinated to the thiol groups, which not only resulted in a positive charge on the single Pt atoms, but also helped to stabilize them against aggregation and leaching.

Recently, Wang *et al.* constructed a Pd^{II}@PDMS single-atom catalyst for the oxidative coupling of benzene to synthesize biphenyl compounds using O_2 as the terminal oxidant with only H_2O as a by-product [88]. In this catalyst, the porous organic copolymer PDMS (a copolymer of divinylbenzene, maleic anhydride and p-styrene sulfonate) containing abundant carboxylic acid and sulfonate groups was used as the support for anchoring single Pd atoms. In the oxidative coupling reaction of benzene, a 26.1% yield of biphenyl with a high selectivity of 98.3% was obtained after 4 h at 120°C, affording a TON value of 363. Under the optimized reaction conditions, an even higher TON of 487 was obtained, which surpassed those achieved on $Pd(OAc)_2$ and other reported heterogeneous catalysts. Benzene, toluene, o-xylene, m-xylene and p-xylene were also good substrates, and the corresponding products were obtained with high selectivity (90.8–97.6%) and yields (10.3–30.8%). Hot filtration experiment results revealed that the reaction did not proceed after the catalyst was removed, thus ruling out the possible contribution of leached Pd to the catalysis. The bidentate –COOH in the Pd^{II}@PDMS catalyst contributed greatly to the stabilization of Pd(II) against reduction as well as the subsequent catalytic activity; in contrast, for catalysts with both $–SO_3H$ and mono-carboxylic groups, or those possessing solely –COOH or $–SO_3H$ groups, much lower yields (0.2–14.2%) were obtained because of their weaker ability to stabilize Pd(II). Evidently, the isolated Pd(II) species was the active site for this reaction.

STABILITY OF SACS

One of the greatest concerns regarding the use of SACs for liquid-phase reactions is their stability. Generally, leaching (the detachment of the single atoms from the support) and aggregation (the formation of clusters and NPs from the single atoms through migration) are the two major factors that severely deteriorate the stability, and the stability of the SACs is strongly dependent on the interaction between the single atoms and the support.

Free single atoms are known to have an extremely high surface energy and therefore cannot be stable. In contrast, upon being fixed on a support, whether on the surface, in the cation position (lattice substitution), confined in a cavity or alloyed with another metal, the single atoms tend to interact strongly with the support via chemical bonding with the donor atoms of the support, such as oxygen or nitrogen atoms or a second metal atom in the case of SAA; these atoms are analogous to the ligands of organometallic complexes. This bonding lowers the surface energy and sometimes even has covalent characteristics [9]. The strong ionic or covalent bonding of the single atoms with the support significantly improves their stability against leaching and/or aggregation. Here, we provide several examples that demonstrate the superior stability of SACs in biomass conversions.

The transformation of biomass into fuels and value-added chemicals is an important and active research area. Biomass-related hydrogenation/hydrodeoxygenation reactions often require harsh reaction conditions, such as elevated hydrogen pressure, moderate to high reaction temperatures and hot water or even acidic reaction media. For example, in the hydrogenation of levulinic acid (LA) to γ-valerolactone (GVL), commercially available Ru/C has proven to be highly active and selective. However, it suffers from severe deactivation under hydrothermal and/or acidic reaction conditions due to Ru leaching [89]. Wang, Zhang and coworkers reported a single-atom Ru/ZrO_2@C (0.85 wt%) catalyst that was highly active and ultra-stable for the hydrogenation reaction of LA [90]. When the reaction was performed in water, the conversion of LA dropped from 69.2% in the first run to 40% in the third cycle on Ru/C, whereas the conversion remained unchanged even after six runs over Ru/ZrO_2@C. The stability of Ru/ZrO_2@C was further demonstrated under harsher conditions (pH = 1); the LA conversion decreased from 77.7 to 25% on Ru/C after three runs, whereas no apparent drop of activity was observed over Ru/ZrO_2@C. ICP-AES results indicated that 14.8 and 7.4% of the Ru leached into acid media and H_2O for Ru/C, respectively, which caused the severe deactivation of the catalyst. In contrast, no leaching of Ru was detected for Ru/ZrO_2@C, which was attributed to the strong interaction between Ru and ZrO_2. Similar results were also reported by other groups [91], although the unambiguous identification of single atoms of Ru on ZrO_2 remains a challenge due to the similar atomic numbers of the two elements.

Another class of ultra-stable SACs are the M–N–C catalysts, in which M is exclusively dispersed as single atoms and bonds with the nearby N atoms to form $M–N_x$ active sites. The $M–N_x$ structure is expected to be highly resistant against high-temperature aggregation and acid leaching based on the strong bonding between the M cation and N

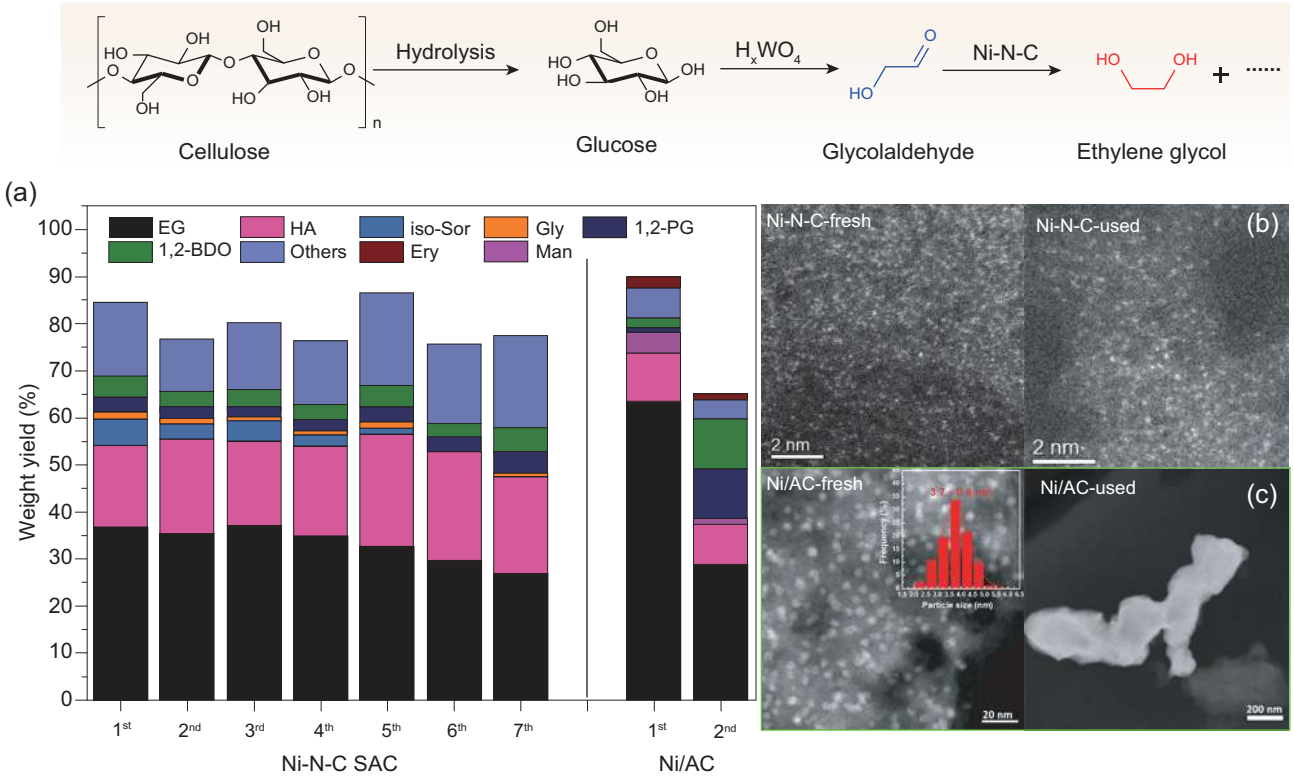

Figure 9. (a) Stability tests of the Ni–N–C catalyst and Ni/AC catalyst, and HAADF-STEM images of fresh and used (b) Ni–N–C and (c) Ni/AC catalysts. Adapted with permission from [13].

atoms. As expected, Wang, Li and coworkers recently reported an ultra-stable Ni–N–C SAC with a Ni loading of 7.5 wt% that exhibited excellent performance in the one-pot conversion of cellulose to EG [13], which is an important reaction for the valorization of biomass to value-added chemicals [92–94]. The Ni–N–C SAC exhibited superior stability compared to its Ni/AC NP counterpart under relatively harsh reaction conditions (245°C, 60 bar H_2, presence of tungstic acid in hot water); it could be recycled seven times without any deactivation, while the Ni/AC lost half of its initial activity during the second run (Fig. 9). Characterizations of the used catalysts showed severe agglomeration of the Ni nanoparticles whereas the Ni–N–C catalyst maintained atomic dispersion. In another biomass-valorization reaction, an MoS_2 monolayer doped with single-atom Co was reported to show superior activity and stability for the hydrodeoxygenation of 4-methylphenol to toluene [95], which is a model reaction for lignin transformations [96]. The single Co atoms were believed to fill S-atom vacancies to be immobilized as a part of the basal plane. The durability was greatly improved—that is, the catalysts could be reused at least seven times for a total reaction time of 56 h without decay in their activity and selectivity; moreover, no sulfur detachment was detected by ICP-AES. This work demonstrated that, when single atoms—100% dispersion of active metal—meet with single layer sheets—the ultimate exfoliation of 2D materials—powerful catalysts can be created.

The above examples, among others, clearly demonstrate that single atoms that are strongly chemically bonded with the donor atoms of the support can behave even more stably than NPs in certain reactions.

CONCLUSION AND PERSPECTIVE

SACs are of great interest and importance for the development of a new generation of low-cost, efficient and robust catalysts. Especially in the field of the green synthesis of fine chemicals, various SACs have been fabricated, and their catalytic potentials have been exploited in a variety of organic transformations, including, but not limited to, selective hydrogenation, oxidation, hydrogenolysis, hydrodeoxygenation, hydroformylation and C–C coupling reactions. In particular, some reactions that represent very important industrial processes, such as the hydrogenolysis of glycerol to 1,3-propanediol and the hydroformylation of propene, would be

very profitable if efficient and robust SACs could be successfully exploited. Traditional homogeneous or heterogeneous NP catalysts involve compromises in terms of activity, selectivity or recyclability. SACs integrate the merits of both these types of catalysts—that is, the unsaturated coordination environment of the single atoms imparts superior catalytic activity per metal atom; the uniform structure of the SACs results in unparalleled selectivity for the desired products; and strong covalent or electronic interactions with the support or another metal provide excellent stability under liquid-phase operating conditions. Therefore, in the field of green chemical synthesis, one can expect further progress in the use of SACs to bridge homogeneous and heterogeneous catalysis.

In spite of its exciting and encouraging beginning, the SAC field is still in its infancy. The following issues must be addressed to obtain an in-depth understanding of single-atom catalysis and eventually achieve the rational design of SACs for specific organic transformations.

(1) The role of the support must be further clarified. In SACs, the single atoms of the active metal interact strongly with the support, and the support serves as the ligands of the active metal centers, just as in homogeneous organometallic molecules. Therefore, the properties of the support can greatly affect the chemical state and coordination structure of the single atoms, and thus their ultimate catalytic performance. By tuning the properties of the support, for example, by grafting functional groups onto the support surface or changing the concentration of defect sites via thermal treatment, the electronic and geometric properties of the central single metal atoms can be changed, providing an effective way to tune the catalytic performance of the SACs. The single atoms may be located in the cation vacancies, the anion vacancies or atop the cation sites of the oxide/sulfide support, which results in different local structures around the single central single atoms, and thus different catalytic performance. For example, in the Co_1/MoS_2 catalyst developed by Tsang *et al.* [95], DFT calculations revealed that, when the Co single atom was located in the sulfur vacancies within the MoS_2 monolayer, the catalyst exhibited the highest stability. In addition, the support may directly participate in the reaction in concert with the single atoms. In such cases, the choice and the modification of the support become key factors in the success of the targeted reaction. Therefore, the elucidation of the multifarious roles played by the support will definitely help to develop an understanding the mechanism of single-atom catalysis and to develop efficient and robust SACs for green chemical synthesis.

(2) Multifunctional SACs should be developed. The green synthesis of fine chemicals calls for the combination of multi-step syntheses into one-pot tandem (domino) reactions. Thus, great effort should be devoted to the development of SACs with multiple functions; for example, the development of a dehydration–hydrogenation bi-functional catalyst through the use of an acidic support might be explored [44,45].

(3) Construction of SACs with a high surface density of the active metal species must be achieved. In order to ensure atomic dispersion, most of the SACs reported to date have had rather low surface densities of the active species (e.g. <0.5 wt%), which leads to a low-volume productivity, although the atom utilization is maximized. For practical applications, SACs with a high surface density of the active metal species are required; this can be accessed by engineering the metal–support interaction. The fabrication of support materials with a high density of defect sites will be favorable considering that the single atoms are usually anchored to the defect sites of the support (vacancies, coordination-unsaturated sites, etc.). For example, in the Pt/WO_x system [44,45,97], the mesoporous WO_x prepared by the alcoholysis method is rich in oxygen vacancies, which allows the Pt species interact strongly with the support and thereby be dispersed as single/pseudo single atoms even at a high loading of ∼2.6 wt%. Nano-engineering of the support is another useful strategy to create abundant surface defects. When the support material is downsized to the nanoscale, both the surface area and density of defect sites will increase greatly, which should be favorable to the incorporation of more single atoms of the active metal. Typical examples include graphene-supported-Fe [17], MoS_2-monolayer-confined Co [95], CoO-nanosheet-supported Rh [80] and TiO_2-nanosheet-anchored Pd [42], all of which feature a practically high density of single atoms. Furthermore, because these 2D materials have distinct physical and chemical properties from their bulk counterparts, they might provide unique catalytic performance when loaded with single atoms. In some cases, doping heteroatoms into the support has also been found to be effective to stabilize a high density of single atoms. For example, the sodium cations in the $Pt–Na/FeO_x$ SACs were found to enhance the dispersion and stabilization of Pt single atoms with a high loading (2.16 wt%) [32]; doping N atoms into carbon sheets can be effective to achieve a high loading of single Co (3.6 wt%) [12], Fe (1.0 wt%) [16] and Ni (7.5 wt%) [13] atoms.

Lastly, more *in situ* characterization techniques should be developed to monitor the dynamic structure of single atoms under operating conditions, as

this would be helpful for the understanding of the catalytic mechanism of SACs and the development of more efficient and robust SACs for the green synthesis of fine chemicals. Operando characterization is particularly challenging for liquid-phase reactions due to the involvement of solvent molecules, but it is of vital importance to efforts to establish a bridge between homogeneous and heterogeneous catalysis by the use of SACs.

FUNDING

This work was supported by the National Natural Science Foundation of China (21373206, 21690080, 21690084, 21503219 and 21673228), the Strategic Priority Research Program of the Chinese Academy of Sciences (XDB17020100) and the National Key Projects for Fundamental Research and Development of China (2016YFA0202801).

REFERENCES

1. Pollak P. *Fine Chemicals: the Industry and the Business*. Hoboken: John Wiley & Sons, 2011.
2. Joshi SS and Ranade VV. *Industrial Catalytic Processes for Fine and Specialty Chemicals*. Amsterdam: Elsevier, 2016.
3. Merino E. Synthesis of azobenzenes: the coloured pieces of molecular materials. *Chem Soc Rev* 2011; **40**: 3835–53.
4. Blaser HU, Steiner H and Studer M. Selective catalytic hydrogenation of functionalized nitroarenes: an update. *Chem Cat Chem* 2009; **1**: 210–21.
5. Polshettiwar V and Varma RS. Green chemistry by nano-catalysis. *Green Chem* 2010; **12**: 743–54.
6. Trost BM. Atom economy—a challenge for organic synthesis: homogeneous catalysis leads the way. *Angew Chem Int Ed Engl* 1995; **34**: 259–81.
7. Beller M, Cornils B and Frohning CD *et al.* Progress in hydroformylation and carbonylation. *J Mol Catal A* 1995; **104**: 17–85.
8. Qiao B, Wang A and Yang X *et al.* Single-atom catalysis of CO oxidation using Pt_1/FeO_x. *Nat Chem* 2011; **3**: 634–41.
9. Yang X, Wang A and Qiao B *et al.* Single-atom catalysts: a new frontier in heterogeneous catalysis. *Acc Chem Res* 2013; **46**: 1740–8.
10. Wei H, Liu X and Wang A *et al.* FeO_x-supported platinum single-atom and pseudo-single-atom catalysts for chemoselective hydrogenation of functionalized nitroarenes. *Nat Commun* 2014; **5**: 5634.
11. Lang R, Li T and Matsumura D *et al.* Hydroformylation of olefins by a rhodium single-atom catalyst with activity comparable to $RhCl(PPh_3)_3$. *Angew Chem Int Ed* 2016; **55**: 16054–8.
12. Liu W, Zhang L and Yan W *et al.* Single-atom dispersed Co–N–C catalyst: structure identification and performance for hydrogenative coupling of nitroarenes. *Chem Sci* 2016; **7**: 5758–64.
13. Liu W, Chen Y and Qi H *et al.* Ultra-durable Ni—N—C single-atom catalyst for biomass conversion under harsh conditions. *Angew Chem Int Ed* 2018; **57**: 7071–5.
14. Xie J, Yin K and Serov A *et al.* Selective aerobic oxidation of alcohols over atomically-dispersed non-precious metal catalysts. *Chem Sus Chem* 2017; **10**: 359–62.
15. Li M, Wu S and Yang X *et al.* Highly efficient single atom cobalt catalyst for selective oxidation of alcohols. *Appl Catal A Gen* 2017; **543**: 61–6.
16. Liu W, Zhang L and Liu X *et al.* Discriminating catalytically active FeNx species of atomically dispersed Fe-N-C catalyst for selective oxidation of the C-H bond. *J Am Chem Soc* 2017; **139**: 10790–8.
17. Deng D, Chen X and Yu L *et al.* A single iron site confined in a graphene matrix for the catalytic oxidation of benzene at room temperature. *Sci Adv* 2015; **1**: e1500462.
18. Zhang M, Wang YG and Chen W *et al.* Metal (hydr) oxides@ polymer core-shell strategy to metal single-atom materials. *J Am Chem Soc* 2017; **139**: 10976–9.
19. Wang A, Li J and Zhang T. Heterogeneous single-atom catalysis. *Nat Rev Chem* 2018; **2**: 65–81.
20. Liu J. Catalysis by supported single metal atoms. *ACS Catal* 2017; **7**: 34–59.
21. Qin R, Liu P and Fu G *et al.* Strategies for stabilizing atomically dispersed metal catalysts. *Small Methods* 2018; **2**: 1700286.
22. Zhang H, Liu G and Shi L *et al.* Single-atom catalysts: emerging multifunctional materials in heterogeneous catalysis. *Adv Energy Mater* 2018; **8**: 1701343.
23. Asokan C, DeRita L and Christopher P. Using probe molecule FTIR spectroscopy to identify and characterize Pt-group metal based single atom catalysts. *Chin J Catal* 2017; **38**: 1473–80.
24. Han B, Lang R and Qiao B *et al.* Highlights of the major progress in single-atom catalysis in 2015 and 2016. *Chin J Catal* 2017; **38**: 1498–507.
25. Nishimura S. *Handbook of Heterogeneous Catalytic Hydrogenation for Organic Synthesis*. New York: Wiley, 2001.
26. Downing RS, Kunkeler PJ and van Bekkum H. Catalytic syntheses of aromatic amines. *Catal Today* 1997; **37**: 121–36.
27. Ren Y, Wei H and Yin G *et al.* Oxygen surface groups of activated carbon steer the chemoselective hydrogenation of substituted nitroarenes over nickel nanoparticles. *Chem Commun* 2017; **53**: 1969–72.
28. Siegrist U, Baumeister P and Blaser HU *et al. Chemical Industries*. New York: Marcel Dekker, 1998, 207–20.
29. Corma A, Serna P and Concepcioón P *et al.* Transforming nonselective into chemoselective metal catalysts for the hydrogenation of substituted nitroaromatics. *J Am Chem Soc* 2008; **130**: 8748–53.
30. Zhai Y, Pierre D and Si R *et al.* Alkali-stabilized Pt-OH_x species catalyze low-temperature water-gas shift reactions. *Science* 2010; **329**: 1633–6.
31. Yang M, Li S and Wang Y *et al.* Catalytically active Au-$O(OH)_x$-species stabilized by alkali ions on zeolites and mesoporous oxides. *Science* 2014; **346**: 1498–501.
32. Wei H, Ren Y and Wang A *et al.* Remarkable effect of alkalis on the chemoselective hydrogenation of functionalized nitroarenes over high-loading Pt/FeO_x catalysts. *Chem Sci* 2017; **8**: 5126–31.

33. Xu G, Wei H and Ren Y *et al.* Chemoselective hydrogenation of 3-nitrostyrene over a Pt/FeO_x pseudo-single-atom-catalyst in CO_2-expanded liquids. *Green Chem* 2016; **18**: 1332–8.
34. Zhang S, Chang CR and Huang ZQ *et al.* High catalytic activity and chemoselectivity of sub-nanometric Pd clusters on porous nanorods of CeO_2 for hydrogenation of nitroarenes. *J Am Chem Soc* 2016; **138**: 2629–37.
35. Corma A and Serna P. Chemoselective hydrogenation of nitro compounds with supported gold catalysts. *Science* 2006; **313**: 332–4.
36. Wang L, Guan E and Zhang J *et al.* Single-site catalyst promoters accelerate metal-catalyzed nitroarene hydrogenation. *Nat Commun* 2018; **9**: 1362.
37. Makosch M, Sá J and Kartusch C *et al.* Hydrogenation of nitrobenzene over Au/MeOx catalysts-a matter of the support. *Chem Cat Chem* 2012; **4**: 59–63.
38. Zitolo A, Goellner V and Armel V *et al.* Identification of catalytic sites for oxygen reduction in iron- and nitrogen-doped graphene materials. *Nat Mater* 2015; **14**: 937–42.
39. Westerhaus FA, Jagadeesh RV and Wienhöfer G *et al.* Heterogenized cobalt oxide catalysts for nitroarene reduction by pyrolysis of molecularly defined complexes. *Nat Chem* 2013; **5**: 537–43.
40. Jagadeesh RV, Surkus AE and Junge H *et al.* Nanoscale Fe_2O_3-based catalysts for selective hydrogenation of nitroarenes to anilines. *Science* 2013; **342**: 1073–6.
41. Zhang L, Wang A and Wang W *et al.* Co-N-C catalyst for C-C coupling reactions: on the catalytic performance and active sites. *ACS Catal* 2015; **5**: 6563–72.
42. Liu P, Zhao Y and Qin R *et al.* Photochemical route for synthesizing atomically dispersed palladium catalysts. *Science* 2016; **352**: 797–800.
43. Zhang B, Asakura H and Zhang J *et al.* Stabilizing a $platinum_1$ single-atom catalyst on supported phosphomolybdic acid without compromising hydrogenation activity. *Angew Chem Int Ed* 2016; **55**: 8319–23.
44. Wang J, Zhao X and Lei N *et al.* Hydrogenolysis of glycerol to 1,3-propanediol under low hydrogen pressure over WO_x-supported single/pseudo-single atom Pt catalyst. *Chem Sus Chem* 2016; **9**: 784–90.
45. Zhao X, Wang J and Yang M *et al.* Selective hydrogenolysis of glycerol to 1,3-propanediol: manipulating the frustrated lewis pairs by introducing gold to Pt/WO_x. *Chem Sus Chem* 2017; **10**: 819–24.
46. Stephan DW. Frustrated Lewis pairs: from concept to catalysis. *Acc Chem Res* 2015; **48**: 306–16.
47. Kyriakou G, Boucher MB and Jewell AD *et al.* Isolated metal atom geometries as a strategy for selective heterogeneous hydrogenations. *Science* 2012; **335**: 1209–12.
48. Pei GX, Liu XY and Wang A *et al.* Promotional effect of Pd single atoms on Au nanoparticles supported on silica for the selective hydrogenation of acetylene in excess ethylene. *New J Chem* 2014, **38**: 2043–51.
49. Pei GX, Liu XY and Wang A *et al.* Ag alloyed Pd single-atom catalysts for efficient selective hydrogenation of acetylene to ethylene in excess ethylene. *ACS Catal* 2015; **5**: 3717–25.
50. Pei GX, Liu XY and Yang X *et al.* Performance of Cu-alloyed Pd single-atom catalyst for semihydrogenation of acetylene under simulated front-end conditions. *ACS Catal* 2017; **7**: 1491–500.
51. Zhou H, Yang X and Li L *et al.* PdZn intermetallic nanostructure with Pd-Zn-Pd ensembles for highly active and chemoselective semi-hydrogenation of acetylene. *ACS Catal* 2016; **6**: 1054–61.
52. Feng Q, Zhao S and Wang Y *et al.* Isolated single-atom Pd sites in intermetallic nanostructures: high catalytic selectivity for semihydrogenation of alkynes. *J Am Chem Soc* 2017; **139**: 7294–301.
53. Lucci FR, Liu J and Marcinkowski MD *et al.* Selective hydrogenation of 1,3-butadiene on platinum–copper alloys at the single-atom limit. *Nat Commun* 2015; **6**: 8550.
54. Yan H, Cheng H and Yi H *et al.* Single-atom Pd_1/graphene catalyst achieved by atomic layer deposition: remarkable performance in selective hydrogenation of 1,3-butadiene. *J Am Chem Soc* 2015; **137**: 10484–7.
55. Huang X, Xia Y and Cao Y *et al.* Enhancing both selectivity and coking-resistance of a single-atom Pd_1/C_3N_4 catalyst for acetylene hydrogenation. *Nano Res* 2017; **10**: 1302–12.
56. Vilé G, Albani D and Nachtegaal M *et al.* A stable single-site palladium catalyst for hydrogenations. *Angew Chem Int Ed* 2015; **54**: 11265–9.
57. Hackett SFJ, Brydson RM and Gass MH *et al.* High-activity, single-site mesoporous Pd/Al_2O_3 catalysts for selective aerobic oxidation of allylic alcohols. *Angew Chem Int Ed* 2007; **46**: 8593–6.
58. Li T, Liu F and Tang Y *et al.* Maximizing the number of interfacial sites in single-atom catalysts for the highly selective, solvent-free oxidation of primary alcohols. *Angew Chem Int Ed* 2018; **57**: 7795–9.
59. Zhang H, Watanabe T and Okumura M *et al.* Catalytically highly active top gold atom on palladium nanocluster. *Nat Mater* 2012; **11**: 49–52.
60. Xie S, Tsunoyama H and Kurashige W *et al.* Enhancement in aerobic alcohol oxidation catalysis of Au_{25} clusters by single Pd atom doping. *ACS Catal* 2012; **2**: 1519–23.
61. Song G, Wang F and Li X. C–C, C–O and C–N bond formation via rhodium(iii)-catalyzed oxidative C–H activation. *Chem Soc Rev* 2012; **41**: 3651–78.
62. Sahu S and Goldberg DP. Activation of dioxygen by iron and manganese complexes: a heme and nonheme perspective. *J Am Chem Soc* 2016; **138**: 11410–28.
63. Chandrasekhar V, Boomishankar R and Nagendran S. Recent developments in the synthesis and structure of organosilanols. *Chem Rev* 2004; **104**: 5847–910.
64. Chen Z, Zhang Q and Chen W *et al.* Single-site Au^I catalyst for silane oxidation with water. *Adv Mater* 2018; **30:** 1704720.
65. Li W, Wang A and Yang X *et al.* Au/SiO_2 as a highly active catalyst for the selective oxidation of silanes to silanols. *Chem Commun* 2012; **48**: 9183–5.
66. Franke R, Selent D and Boörner A. Applied hydroformylation. *Chem Rev* 2012; **112**: 5675–732.
67. Evans D, Osborn JA and Wilkinson G. Hydroformylation of alkenes by use of rhodium complex catalysts. *J Chem Soc, A* 1968; 3133–42.
68. Ford ME and Premecz JE. Preparation and evaluation of ion exchange resin-immobilized rhodium-phosphine hydroformylation catalysts. *J Mol Catal* 1983; **19**: 99–112.
69. Li C, Wang W and Yan L *et al.* A mini review on strategies for heterogenization of rhodium-based hydroformylation catalysts. *Front Chem Sci Eng* 2018; **12**: 113–23.
70. Sun Q, Dai Z and Meng X *et al.* Enhancement of hydroformylation performance via increasing the phosphine ligand concentration in porous organic polymer catalysts. *Catal Today* 2017; **298**: 40–5.
71. Sun Q, Dai Z and Meng X *et al.* Task-specific design of porous polymer heterogeneous catalysts beyond homogeneous counterparts. *ACS Catal* 2015; **5**: 4556–67.
72. Jiang M, Yan L and Ding Y *et al.* Ultrastable 3V-PPh_3 polymers supported single Rh sites for fixed-bed hydroformylation of olefins. *J Mol Catal A: Chem* 2015; **404**: 211–7.
73. Li C, Yan L and Lu L *et al.* Single atom dispersed Rh-biphephos&PPh_3@porous organic copolymers: highly efficient catalysts for continuous fixed-bed hydroformylation of propene. *Green Chem* 2016; **18**: 2995–3005.
74. Huang L and Kawi S. An active and stable Wilkinson's complex-derived SiO_2-tethered catalyst via an amine ligand for cyclohexene hydroformylation. *Catal Lett* 2004; **92**: 57–62.

75. van der Veen LA, Keeven PH and Schoemaker GC *et al*. Origin of the bite angle effect on rhodium diphosphine catalyzed hydroformylation. *Organometallics* 2000; **19**: 872–83.
76. Billig E, Abatjoglou AG and Bryant DR. (Union Carbide Corp.) Bis-phosphite compounds. 1987; Eur. Pat. EP0213639.
77. Billig E, Abatjoglou AG and Bryant DR. (Union Carbide Corp.) Bis-phosphite compounds. 1988; US Pat. 4748261.
78. Li C, Sun K and Wang W *et al*. Xantphos doped Rh/POPs-PPh_3 catalyst for highly selective long-chain olefins hydroformylation: chemical and DFT insights into Rh location and the roles of Xantphos and PPh_3. *J Catal* 2017; **353**: 123–32.
79. Liu J, Yan L and Ding Y *et al*. Promoting effect of Al on tethered ligand-modified Rh/SiO_2 catalysts for ethylene hydroformylation. *Appl Catal, A* 2015; **492**: 127–32.
80. Wang L, Zhang W and Wang S *et al*. Atomic-level insights in optimizing reaction paths for hydroformylation reaction over Rh/CoO single-atom catalyst. *Nat Commun* 2016; **7**: 14036.
81. Liu X, Hu B and Fujimoto K *et al*. Hydroformylation of olefins by Au/Co_3O_4 catalysts. *Appl Catal, B* 2009; **92**: 411–21.
82. Miyaura N, Yanagi T and Suzuki A. The palladium-catalyzed cross-coupling reaction of phenylboronic acid with haloarenes in the presence of bases. *Synth Commun* 1981; **11**: 513–9.
83. Heck RF. Palladium-catalyzed vinylation of organic halides. *Org React* 1982; **27**: 345–90.
84. Stork G, Rosen P and Goldman NL. The α-alkylation of enolates from the lithium-ammonia reduction of α, β-unsaturated ketones. *J Am Chem Soc* 1961; **83**: 2965–6.
85. Zhang L, Wang A and Miller JT *et al*. Efficient and durable Au alloyed Pd single-atom catalyst for the Ullmann reaction of aryl chlorides in water. *ACS Catal* 2014; **4**: 1546–53.
86. Zhang X, Sun Z and Wang B *et al*. C-C coupling on single-atom based heterogeneous catalyst. *J Am Chem Soc* 2018; **140**: 954–62.
87. Lee EK, Park SA and Woo H *et al*. Platinum single atoms dispersed on carbon nanotubes as reusable catalyst for Suzuki coupling reaction. *J Catal* 2017; **352**: 388–93.
88. Liu Y, Zhou Y and Li J *et al*. Direct aerobic oxidative homocoupling of benzene to biphenyl over functional porous organic polymer supported atomically dispersed palladium catalyst. *Appl Catal B* 2017; **209**: 679–88.
89. Yan Z, Lin L and Liu S. Synthesis of γ-valerolactone by hydrogenation of biomass-derived levulinic acid over Ru/C catalyst. *Energy Fuels* 2009; **23**: 3853–8.
90. Cao W, Luo W and Ge H *et al*. UiO-66 derived Ru/ZrO_2@C as a highly stable catalyst for hydrogenation of levulinic acid to γ-valerolactone. *Green Chem* 2017; **19**: 2201–11.
91. Ftouni J, Munñoz-Murillo A and Goryachev A *et al*. ZrO_2 is preferred over TiO_2 as support for the Ru-catalyzed hydrogenation of levulinic acid to γ-valerolactone. *ACS Catal* 2016; **6**: 5462–72.
92. Ji N, Zhang T and Zheng M *et al*. Direct catalytic conversion of cellulose into ethylene glycol using nickel-promoted tungsten carbide catalysts. *Angew Chem* 2008; **120**: 8638–41.
93. Pang J, Zheng M and Sun R *et al*. Synthesis of ethylene glycol and terephthalic acid from biomass for producing PET. *Green Chem* 2016; **18**: 342–59.
94. Wang A and Zhang T. One-pot conversion of cellulose to ethylene glycol with multifunctional tungsten-based catalysts. *Acc Chem Res* 2013; **46**: 1377–86.
95. Liu G, Robertson AW and Li MMJ *et al*. MoS_2 monolayer catalyst doped with isolated Co atoms for the hydrodeoxygenation reaction. *Nat Chem* 2017; **9**: 810–6.
96. Li C, Zhao X and Wang A *et al*. Catalytic transformation of lignin for the production of chemicals and fuels. *Chem Rev* 2015; **115**: 11559–624.
97. Yang M, Zhao X and Ren Y *et al*. Pt/Nb-WO_x for the chemoselective hydrogenolysis of glycerol to 1,3-propanediol: Nb dopant pacifying the over-reduction of WO_x supports. *Chin J Catal* 2018; **39**: 1027–37.